Protective effects of recombinant 53-kDa protein of *Trichinella spiralis* on acute lung injury in mice via alleviating lung pyroptosis by promoting M2 macrophage polarization

Ling-yu Wei[1],*, An-qi Jiang[1],*, Ren Jiang[1], Si-ying Duan[1], Xue Xu[1], Ze-da-zhong Su[2] and Jia Xu[1] [iD]

Abstract

Trichinella spiralis represents an effective treatment for autoimmune and inflammatory diseases. The effects of recombinant *T. spiralis* (TS) 53-kDa protein (rTsP53) on acute lung injury (ALI) remain unclear. Here, mice were divided randomly into a control group, LPS group, and rTsP53 + LPS group. ALI was induced in BALB/c mice by LPS (10 mg/kg) injected via the tail vein. rTsP53 (200 μl; 0.4 μg/μl) was injected subcutaneously three times at an interval of 5 d before inducing ALI in the rTsP53+LPS group. Lung pathological score, the ratio and markers of classic activated macrophages (M1) and alternatively activated macrophages (M2), cytokine profiles in alveolar lavage fluid, and pyroptosis protein expression in lung tissue were investigated. RTsP53 decreased lung pathological score. Furthermore, rTsP53 suppressed inflammation by increasing IL-4, IL-10, and IL-13. There was an increase in alveolar M2 macrophage numbers, with an increase in CD206 and arginase-1-positive cells and a decrease in alveolar M1 markers such as CD197 and iNOS. In addition, the polarization of M2 macrophages induced by rTsP53 treatment could alleviate ALI by suppressing lung pyroptosis. RTsP53 was identified as a potential agent for treating LPS-induced ALI via alleviating lung pyroptosis by promoting M2 macrophage polarization.

Keywords

Acute lung injury, recombinant 53-kDa protein, *Trichinella spiralis*, alternatively activated macrophage, lung pyroptosis

Introduction

Acute lung injury (ALI) is a common and devastating clinical disorder that leads to high mortality in patients in intensive care units.[1] ALI is characterized by uncontrolled inflammation and damage to the air–blood barrier, leading to pulmonary edema, hypoxemia, and potential respiratory failure.[2] Although various therapeutic strategies have been proposed in recent years, outcomes remain unsatisfactory and effective treatment of ALI remains a major challenge.

Numerous inflammatory mediators are released in the early stage of ALI, while suppressive inflammatory mediators are discharged in large amounts in advanced stages. Immune dysfunction secondary to uncontrolled inflammation is a critically important mechanism in the

[1]Emergency Department, The First Affiliated Hospital of Sun Yat-sen University, No.58, Zhongshan 2nd Road, 510080, Guangzhou, China
[2]Guangdong Provincial People's Hospital, Guangdong Academy of Medical Sciences, School of Medicine, South China University of Technology, Guangzhou 510080, China

*Joint first authors.

Corresponding authors:
Jia Xu or Ze-da-zhong Su, The First Affiliated Hospital of Sun Yat-sen University, No.58, Zhongshan 2nd Road, 510080, Guangzhou, China.
Email: xujia5@mail.sysu.edu.cn

Guangdong Provincial People's Hospital, Guangdong Academy of Medical Sciences, School of Medicine, South China University of Technology, Guangzhou 510080, China.
Email: 673946537@qq.com.

development of ALI. Therefore, suppression of early uncontrolled inflammatory responses and improvement of immune dysfunction may provide a new therapeutic strategy for ALI. The lung contains two different populations of macrophages: alveolar and interstitial macrophages, which are closely related to immune dysfunction in ALI. Some studies suggested that macrophages protect the lungs from injury, while others reported that macrophages are associated with the pathogenesis of lung injury.[3] Macrophages connect the innate and acquired immune responses *in vivo*, and thus we hypothesized that the differentiation and functional status of macrophages play an important role in ALI.

Macrophages are a subset of mononuclear cells and function in non-specific immunity. According to their responses to environmental stimuli, macrophages undergo two different types of polarization into the classically activated phenotype (M1) and alternatively activated phenotype (M2).[4] Numerous studies have demonstrated the roles of these two macrophage types in the inflammatory pathway, and their emergence appears to determine the fate of inflammatory signaling and disease progression. More importantly, they exhibit distinct features in terms of ALI. CD197, CD163, and induced NO synthase (iNOS) are markers of M1-polarized macrophages, and M2-polarized macrophages are characterized by CD206 and Arg-1. M1 macrophage polarization is influenced by the microenvironment such as microbial products and cytokines, but when stimulated by interleukin IL-4, IL-10, and IL-13, macrophages differentiate into M2 macrophages. Lu et al.[5] found that M1 macrophages play a critical role in the early stage of ALI. However, M2 macrophages can repair lung tissue by limiting the levels of pro-inflammatory cytokines in the cellular space and produce anti-inflammatory cytokines.[6] Thus, macrophage polarization is closely related to the prognosis of ALI.

Pyroptosis is a type of programmed cell death.[7] Inflammasomes, including NLRP3, are key molecules that initiate the activation of caspase-1, thus accelerating the IL-1β transformation from precursor to maturity and eventually inducing pyroptosis.[8,9] PAMPs, such as LPS, are recognized by the NLRP3 to activate caspase-1, which then promotes the secretion of IL-1β.[10] Furthermore, recent studies have proved that pyroptosis plays a vital role in respiratory diseases.[11] Lung endothelial pyroptosis have been proved closely related to ALI.[12,13] In addition, anti-inflammatory M2 macrophages may reduce inflammation-induced pyroptosis, and then alleviate LPS-induced lung injury.[14,15] Therefore, promoting M2 macrophage polarization may be a promising treatment to reduce ALI via decreasing lung pyroptosis.

Trichinellosis is a major zoonotic parasitosis resulting from the ingestion of raw or undercooked meat infected with the nematodes *Trichinella* spp., particularly in developing countries. Several studies have demonstrated that infection with *Trichinella spiralis* is an effective treatment for autoimmune disease. The excretory–secretory antigens from *T. spiralis* protect hosts from sepsis. Vaccination of mice with trichinellosis induced a Th2 predominant immune response and partial immune protection against challenge infection. *Trichinella* infection increases the M2/M1 ratio in the peritoneal lavage fluid of obese mice.[16] Chen et al. suggested that the *T. spiralis* 53-kDa protein attenuates LPS-induced damage during the pro-inflammatory stage of sepsis_ENREF_1.[17] In previous studies, we showed that recombinant excretory–secretory 53-kDa protein of *T. spiralis* (rTsP53) modulates intestinal epithelial barrier integrity in LPS-induced septic mice. As a result, parasitic immunity shows potential for treating severe infections. However, the relationship between rTsP53 and macrophage-polarization-dependent pyroptosis in LPS-induced ALI is still unknown. Therefore, the aim of this study was to investigate the protective potential and mechanism of rTsP53 in experimental LPS-induced lung injury in mice.

Materials and methods

Cloning, expression, purification, and identification of TsP53

RTsP53 was produced as previously described.[18] Briefly, the TsP53 gene was amplified from a cDNA template extracted from *T. spiralis* larvae using forward primer (CCCCATATGTCTACAGACAATGA GAATG) and reverse primer (ATTCTCGAGGAAC AACAACTGTAGTTC) containing *Nde*I and *Xho*I restriction enzyme sites. The PCR product was purified and cloned into the corresponding restriction sites of pET28a(+) (Novagen, Madison, WI, USA) expression vector. The pET-28a(+)-TsP53 plasmid was transformed into *Escherichia coli* BL21 for large-scale expression of the recombinant protein induced by isopropyl-β-D-thiogalactopyranoside (IPTG, CalBiochem, San Diego, CA, USA) at a final concentration of 1.0 mM for 5 h at 28°C. The expressed protein was purified by immobilized metal affinity chromatography. Finally, the recombinant protein was eluted with 200 mM imidazole, which was separated from the protein sample with a PD-10 column. Endotoxin was removed by AffinityPakTM Detoxi-GelTM Endotoxin Removing Gel (Thermo Scientific, Waltham, MA, USA) until the endotoxin level was <0.1 endotoxin U/ml as determined by the limulus amebocyte lysate assay according to the

manufacturer's protocol. The concentration was determined by Bradford assay. The expression of rTsP53 was visualized by Coomassie brilliant blue G-250 and identified by Western blotting using the serum of Ts-infected mice.

Animals and experimental protocol

Male BALB/c mice (6–8 wk old) were purchased from the experimental animal center of Sun Yat-sen University. Mice were housed in ventilated cages and fed a normal laboratory diet. All animals were maintained under specific pathogen-free conditions at the animal facility, and experiments followed a protocol drafted by the Animal Ethics Committee of Sun Yat-sen University. Mice were divided randomly into three groups: control group ($n = 15$), LPS group ($n = 15$), and rTsP53+LPS group ($n = 15$). Mice were deprived of food for 24 h prior to the induction of ALI by LPS (10 mg/kg, dissolved in 200 μl PBS solution) injected via the tail vein, and then allowed free access to tap water. In the rTsP53+LPS group, mice were treated with rTsP53 (50 μg in 200 μl PBS) or PBS by subcutaneous injection three times at an interval of 5 d before inducing ALI. LPS group mice were injected subcutaneously with 200 μl PBS simultaneously. LPS from *E. coli* 055: B5 was obtained from Sigma-Aldrich (St. Louis, MO, USA).

Ab isotypes of anti-rTsP53

The sera levels of IgG1 and IgG2a from mice in the three groups were measured by ELISA against rTsP53 before LPS injection. Briefly, 96-well flat-bottom microtiter plates (Nunc, Roskilde, Denmark) were coated with 100 μl of rTsP53 at a concentration of 5 μg/ml in 0.1 M carbonate bicarbonate buffer (pH 9.6) per well at 4°C for 10 h and then blocked with 5% skim milk in PBS-T for 2 h at 37°f. Serum samples diluted to 1:100 (IgG1) and 1:100 (IgG2a) with PBS-T containing 0.1% BSA (100 μl/well) were added in duplicate and then incubated for 2 h at 37°C. HRP-conjugated goat anti-mouse IgG1 and IgG2a (100 μl; both 1:2,000, Southern Biotech Co., Birmingham, AL, USA) were incubated for 0.5 h at 37°o and then the color was developed with substrate 3,3′,5,5′-tetramethylbenzidine. The absorbance was measured at 450 nm after adding 2 M H_2SO_4 (50 μl per well) to stop the reaction.

Bronchoalveolar lavage fluid and serum cytokine analysis

Bronchoalveolar lavage fluid (BALF) and serum from animals in different groups were collected at 0, 2, 6, 12, 24, 48, and 72 h after LPS injection and stored at −80°C until further analysis. The levels of IL-4, IL-10, IL-13, TNF-α, IL-6, and IL-1β were measured with an ELISA kit (R&D Systems, Minneapolis, MN, USA) according to the manufacturers' instructions. All samples and standards were measured in duplicate.

Pathological score of the lung tissues

To assess lung damage at 72 h after LPS injection, mice from three different groups were sacrificed by pentobarbital overdose (100 mg/kg). Lung tissues of the left lower lobe were removed. Tissue samples from each animal were fixed, dehydrated, and embedded in paraffin. Tissues were cut to 5-μm sections and mounted on a clean glass at 37°C for 10 h. The sections were cleared, hydrated, and stained with hematoxylin and eosin. Pathological changes in the lung tissue were observed by light microscopy. Pneumonedema, alveoli, interstitial inflammation, pneumorrhagia, atelectasis, and transparent membrane formation were evaluated individually using Smith scores as previously described.[19] The histology damage score was calculated on a 0- to 4-point scale: scope of lesions < 25%, 1; 25–50%, 2; 50–75%, 3; > 75%, 4. The total score was the sum of all items mentioned above. Scoring was conducted in a blinded manner.

Lung wet/dry mass ratio

The lung wet/dry ratio was calculated to assess pneumonedema. After sacrificing the mice, the lungs were surgically dissected from the heart, trachea, and main bronchi. Each lung was rinsed with PBS and weighed to obtain the "wet" mass. Next, the lung specimen was stored at 70°h for 48 h to obtain the "dry" mass.

Preparation of bronchoalveolar macrophages

At 72 h after ALI induction, mice from three different group were sacrificed by pentobarbital overdose (100 mg/kg). After anesthesia, a cervical incision was made immediately, and blunt dissection was performed to expose the trachea. A 14-gauge angiocatheter was inserted into the trachea and sutured to fix it in place. The lung was rinsed by instilling sterile normal saline three times. The effluent was re-collected by gravity drainage. Cells in the alveolar lavage fluid were counted with a hematimeter by light microscopy. Differential cell counts were performed on cytospin preparations using light microscopy on Wright–Geimsa-stained samples. The cells were harvested and centrifuged at 200 *g* for 5 min (Boeco Germany U320 centrifuge, Hamburg, Germany), and then washed twice and resuspended in PBS at a concentration of 10^5 cells per 100 μl for flow cytometry analysis.

FACS analysis

Flow cytometry was performed using prepared cells as described above. FcγR was blocked with anti-CD19/ CD32 mAb 2.4G2 (BD Biosciences Franklin Lakes, NJ, USA) for 20 min. The cells were incubated with 1 µg of primary Ab specific for cell surface markers of the M1 and M2 macrophages on ice avoiding light for 30 min, washed twice with PBS, and then evaluated by flow cytometry. The following Abs were diluted in 1% FBS in PBS: FITC-Anti-F4/80 (0.2 mg/ml), APC-Anti-CD197 (0.2 mg/ml), and FITC-Anti-CD206 (0.05 mg/ ml) (eBiosciences, San Diego, CA, USA). The appropriate fluorochrome-conjugated isotype controls were used for each Ab. Flow cytometry was performed by fluorescence-activated cell sorting (BD Biosciences). Data were collected using Cellquest software (BD Biosciences) and analyzed with FlowJo software (Tree Star, Ashland, OR, USA).

RT-PCR

Total RNA was extracted from bronchoalveolar macrophages with a MiniBEST universal RNA Extraction Kit (9767, Takara, Shiga, Japan) according to the manufacturer's instructions. The mRNA expression levels of TNF-α, iNOS, IL-10, and Arg-1 were measured by RT-PCR performed using a RT-PCR kit (ReverTra Ace qPCR RT Kit FSQ-101, Toyobo, Osaka, Japan) according to the manufacturer's instructions. Gene-specific primers were designed to amplify these markers genes. The reference gene β-actin was used as an endogenous control. The primer sequences were as follows: TNF-α Forward: 5′CCCAGACCCTCACACTCAG ATCAT-3′, Reverse: 5′-GCAGCCTTGTCCCTTGA AG-AGAA-3′; IL-10 Forward: 5′-CTTTCACTTGC CCTCATCC-3′, Reverse: 5′-ACAAAC-AATACGCC ATTCCC-3′; iNOs Forward: 5′-ACATTCAGATCC CGAAACGC-3′, Reverse: 5′-ACAATCCACAACTC GCTCC-3′; Arg-1 Forward: 5′-GGGGAAAGCCAA-GAAG3′, Reverse: 5′TGGTTGTCAGGGGAGTGT-3′; β-actin Forward: 5′-TGGA-ATCCTGTGGCAT CCATGAAAC-3′, Reverse: 5′-TAAAACGCAGCTC AGTAACAGT-CCG -3′. The relative mRNA expression levels of each gene was calculated and analyzed with Image J software (NIH, Bethesda, MD, USA).

Western blot analysis

Lung tissues proteins of different group were harvested with total tissue lysis buffer (Cell Signaling Technology, Danvers, MA, USA). Protein extracts were subjected to SDS-PAGE and transferred to polyvinylidene fluoride membrane (Cell Signaling Technology) at 100 V for 2.5 h. The membrane was blocked with 5% skim milk powder in PBS (pH 7.4)

at 37°C for 1 h. The following Abs were used to detect the expression of pyroptosis proteins: rabbit anti-mouse caspase-1 Ab (1:1000; NOVUS), GSDMD (1:1000; Abcam) and GAPDH (1:10000; Abcam). Proteins were visualized with goat anti-rabbit HRP-conjugated IgG (1:5000; Cell Signaling Technology), followed by analysis of the electrochemiluminescence intensity of immunoreactive bands. The results were expressed as the ratio of total caspase-1 protein to GAPDH and GSDMD protein to GAPDH. The statistical comparisons for Western blot analysis were made relative to non-interference.

Statistical analysis

All values were expressed as the mean $\pm$ SEM. Statistical analysis was performed using SPSS 15.0 software for Windows (SPSS, Inc., Chicago, IL, USA). One-way and two-way analysis of variance was used to compare statistical differences under different conditions. $P < 0.05$ was considered to indicate statistical significance.

Results

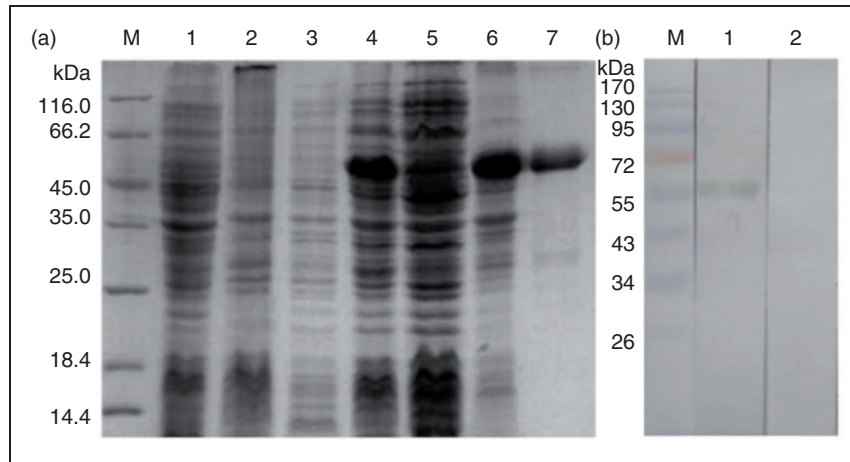## Expression, purification, and identification of rTsP53

The highly expressed fusion protein (Figure 1) was purified at the correct molecular mass. The purified protein was analyzed by SDS-PAGE and identified in the serum from Ts-infected mice, with a single band at the expected size.

## IgG, IgG1, and IgG2a Ab response to rTsP53 protein in mice

Mice immunized with rTsP53 protein without complete Freund adjuvant three times produced high levels of the specific Abs IgG and IgG1, but not IgG2a, compared with naïve normal and mice injected with PBS in terms of the OD value (450 nm) (Figure 2). The rTsP53 + LPS group produced significantly higher levels of rTsP53-specific IgG1 Ab (0.811 ± 0.055) compared with the control group (0.082 ± 0.008) and LPS group (0.095 ± 0.006). The levels of IgG2a against rTsP53 in the three groups were negligible and showed no significant difference among groups.

Microscopic lung damage and pathological score

Lung tissues from mice in the control group (Figure 3a) showed no significant pathological damage, revealing normal microstructures of the pulmonary alveoli and interstitial tissues. Histological damage to the lung tissues in mice from the LPS group (Figure 3b) showed large areas with diffuse infiltration of inflammation

Figure 1. SDS-PAGE (12%) of prokaryotic expression and pET-28a(+)-TsP53 and Western blotting of purified recombinant protein. (a) Expression and purification of rTsP53 in *E. coli* BL21/DE3. M, protein molecular markers. (b) Western blot analysis of rTsP53. M, protein molecular markers.
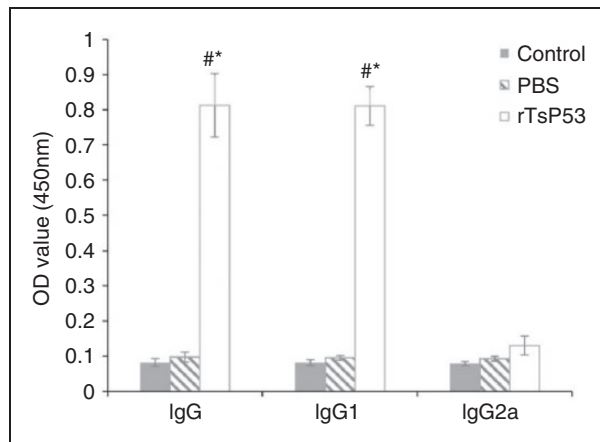
Figure 2. Ab isotype profiles of rTsP53. Results expressed as the means $\pm$ SEM. *$P < 0.05$ vs. control group and #$P < 0.05$ vs. PBS group.

cells, alveoli exudation, thickened alveoli septum, partial alveoli collapse, and formation of a hyaline membrane. Administration of rTsP53 protein resulted in less tissue damage with ameliorated alveoli exudation and interstitial congestion (Figure 3c). rTsP53 also reduced the amount of hyaline membrane and inflammatory cells in the lung tissues. The Smith score (Figure 3d) in the control group was 0.62 ± 0.14. The pathological score of lung tissue in the rTsP53+LPS group was significantly lower than that in the LPS group (3.59 ± 1.24 vs. 7.73 ± 1.97, respectively; $P < 0.05$).

Lung wet/dry mass ratio

The wet/dry mass ratio (Table 1) was determined to assess pulmonary edema. Pneumonedema was

significantly alleviated in the LPS+rTsP53 group at 72 h after ALI induction compared with that in the LPS group, but no difference compared with the control group.

BALF levels of cytokines TNF-α, IL-6, IL-1β, IL-4, IL-10, and IL-13

The concentrations of the cytokines TNF-α (Figure 3e), IL-1β (Figure 3f), IL-6 (Figure 3g), IL-4 (Figure 3h), IL-10 (Figure 3i) and IL-13 (Figure 3j) in the BALF were measured in the three groups of mice at 0, 2, 6, 12, 24, 48, and 72 h after LPS injection. A systemic increase in pro-inflammatory cytokines is a characteristic response during the process of ALI. In the LPS group, the TNF-α, IL-1β, and IL-6 levels in BALF were much higher than those in the control group. However, treatment with rTsP53 significantly attenuated the levels of these pro-inflammatory cytokines induced by LPS injection. Additionally, the anti-inflammatory cytokines IL-4, IL-10, and IL-13, which could induce M2 macrophages, were significantly elevated in the rTsP53+LPS group at all measured times compared with that in the LPS group. These results indicate that rTsP53 inhibits the inflammatory response in the pathogenesis of ALI.

Serum levels of TNF-α, IL-6, IL-1β, IL-4, IL-10, and IL-13

The concentrations of the cytokines TNF-α (Figure 4a), IL-1β (Figure 4b), IL-6 (Figure 4c), IL-4 (Figure 4d), IL-10 (Figure 4e), and IL-13 (Figure 4f) in the serum were measured in the three groups of mice at 0, 2, 6, 12, 24, 48, and 72 h after LPS injection. A systemic increase in pro-inflammatory cytokines is
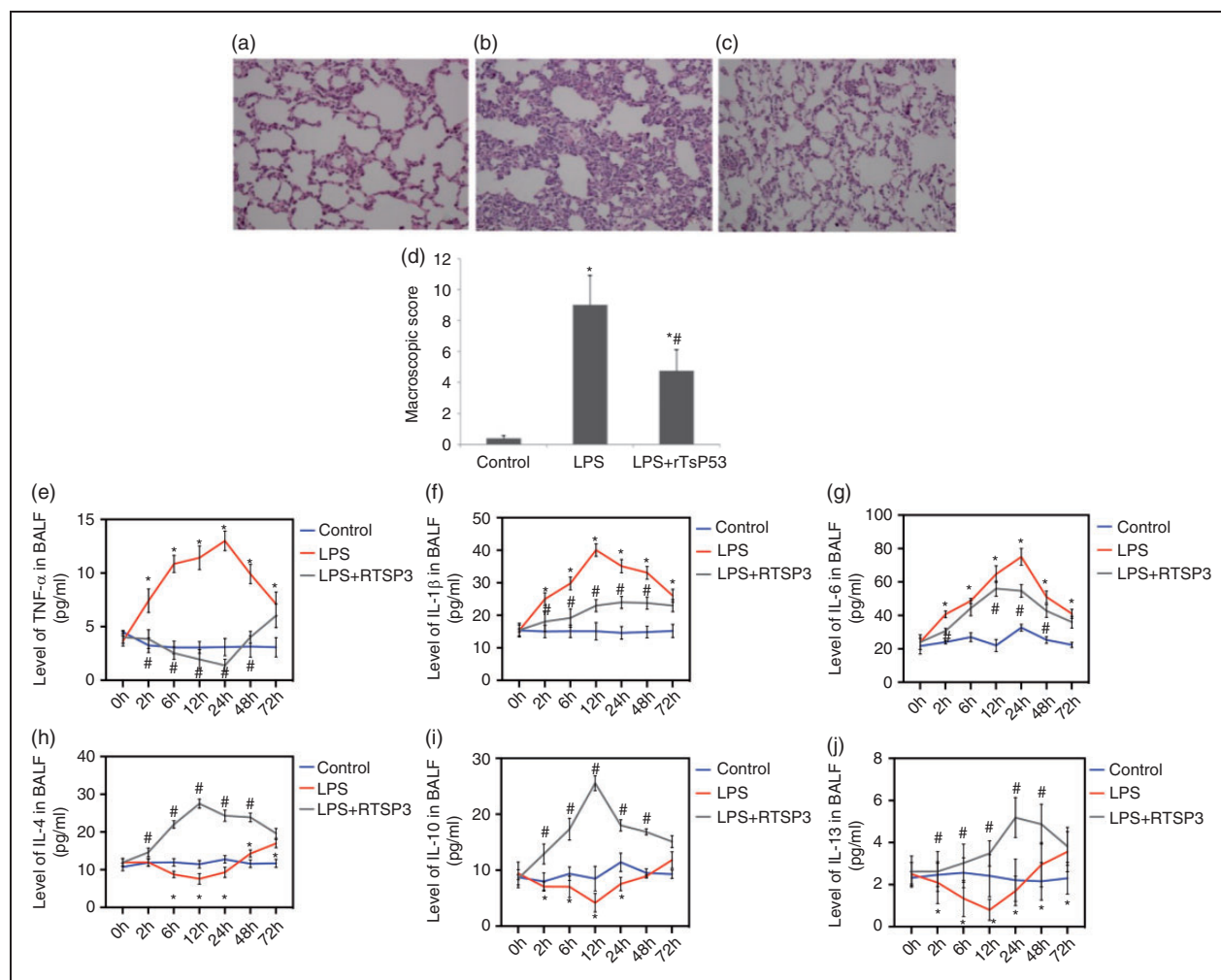
Figure 3. Protective effects of rTsP53 administration on microscopic score in lung tissue from three groups (a: control group; b: LPS group; c: LPS+rTsP53 group). Lung sections were collected at necropsy at 72 h after LPS injection and stained with H&E (magnification, ×200). BALF concentrations of TNF-α (e), IL-1β (f), IL-6(g), IL-4(h), IL-10 (i), and IL-13 (j) in mice at different times in three groups. Data are expressed as means ± SEM. *$P < 0.05$ vs. control group, #$P < 0.05$ vs. LPS group.

Table 1. Comparison of wet/dry mass ratio of lung tissue in three different groups.

| Group	Control	LPS	rTsP53 + LPS
Wet/dry ratio	4.74 ± 0.46	7.03 ± 0.75*	5.09 ± 0.52#

*$P < 0.05$ vs. control group, #$P < 0.05$ vs. LPS group.

a characteristic response during the process of ALI. In the LPS group, the TNF-α, IL-1β, and IL-6 levels in serum were much higher than those in the control group. However, treatment with rTsP53 significantly attenuated the levels of these pro-inflammatory cytokines induced by LPS injection. Additionally, the anti-inflammatory cytokines IL-4, IL-10, and IL-13, which could induce M2 macrophages, were significantly

elevated in the rTsP53+LPS group at all measured times compared with that in the LPS group. These results indicate that rTsP53 inhibits the inflammatory response in the pathogenesis of ALI.

Phenotype of murine BALF macrophages

We examined the expression of surface markers on BALF macrophages from mice in the three different groups at 6 and 24 h following ALI induction to evaluate the effects of rTsP53 on the macrophage phenotype. In the control group, the proportion of FIFC-anti-F4/80(+)/APC-anti-CD197(+) double-positive macrophages (M1) (Figure 5a) was 1.98 ± 0.27% and the proportion of FITC-anti-F4/80(+)/PE-anti-CD206(+) double-positive macrophages (M2)
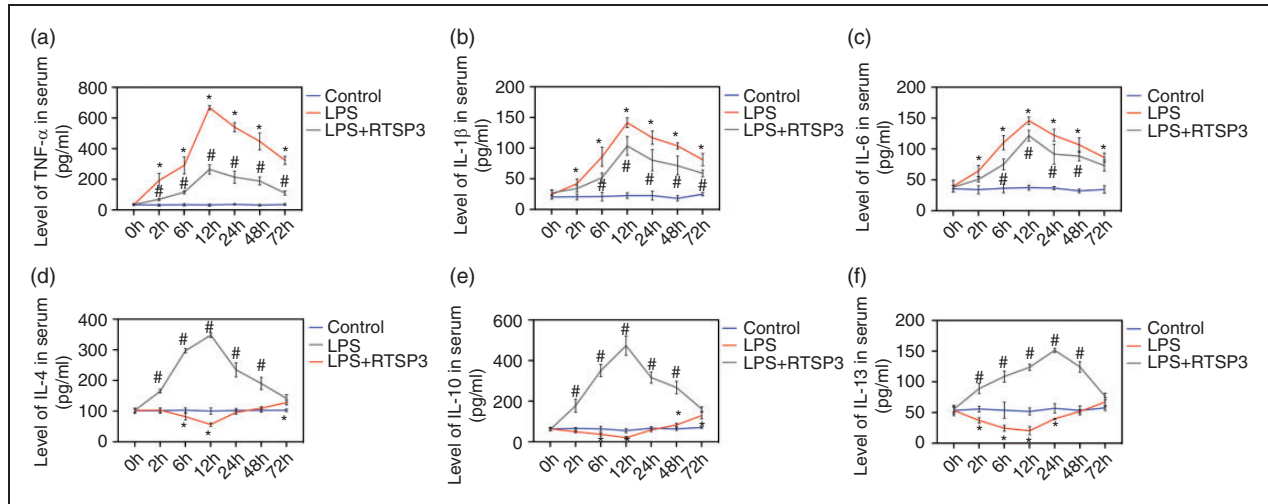
Figure 4. Serum concentrations of TNF-α (a), IL-1β (b), IL-6 (c), IL-4 (d), IL-10 (e), and IL-13 (f) in mice at different times in three groups. Data are expressed as means ± SEM. *$P < 0.05$ vs. control group, #$P < 0.05$ vs. LPS group.

(Figure 5b) was $0.745 \pm 0.31\%$. As predicted, LPS treatment significantly increased the percentage of F4/80(+)/CD197(+) macrophages compared with that in the control group. The proportion of BALF macrophages with the M2 phenotype in the rTsP53+LPS group (Figure 5f) was significantly higher following pre-treatment with rTsP53 protein compared with the LPS group ($6.48 \pm 0.81\%$ vs. $1.60 \pm 0.32\%$, respectively; $P < 0.05$) at 6 h (Figure 5d) after ALI induction. At 24 h after LPS administration, the proportion of M2 macrophages in the rTsP53+LPS group (Figure 5j) further increased and was much higher than that in the LPS group (Figure 5h) ($11.0 \pm 1.34\%$ vs $3.25 \pm 0.46\%$, respectively; $P < 0.05$). Additionally, rTsP53 treatment reduced CD197 (M1 marker) (Figures 5e and i) expression on macrophages compared with the LPS group (Figures 5c and g) at 6 h ($8.33 \pm 0.97\%$ vs $11.0 \pm 1.15\%$, respectively; $P < 0.05$) and at 24 h ($4.39 \pm 0.51\%$ vs $13.60 \pm 1.55\%$, respectively; $P < 0.05$). Next, we examined the mRNA expression of markers (Arg-1 and iNOS) and cytokines (IL-10 and TNF-α) in M1 or M2 macrophages by RT-PCR at 24 h (Figures 5k and l). LPS injection increased the mRNA expression levels of TNF-α and iNOS compared with the control group. rTsP53 treatment in ALI mice up-regulated the expression of the M2 marker Arg-1 and anti-inflammatory cytokine IL-10 while reducing mRNA expression levels of the M1 marker iNOS and pro-inflammatory cytokine TNF-α compared with the LPS group. These results indicate that rTsP53 modulates the polarization of alternatively activated macrophages, switching the BALF macrophages from M1 to M2 in ALI mice induced by LPS administration.

Role of M2 macrophages polarization induced by rTsP53 on lung tissue pyroptosis

In vitro, we examined whether rTsP53 could promote M2 macrophages polarization in mice from the three groups by ELISA to evaluate the effects of rTsP53 on the macrophages' polarization and relationship between the rTsP53 protein and markers of macrophages. *In vivo*, we utilized lung tissue from the three groups harvested at 12, 24, and 48 h after ALI induction. In the control group (Figures 6a and c), pyroptosis proteins caspase-1 and GSDMD expression remained relatively low at 12, 24, and 48 h. LPS significantly increased expression of pyroptosis proteins in LPS-induced ALI mice at 12, 24, and 48 h (Figures 6a and c]. The highest expression of caspase-1 and GSDMD were observed at 24 h in the LPS group. After rTsP53 administration, the expression of pyroptosis proteins was reduced in ALI mice compared with that in those treated with LPS alone at 12, 24, and 48 h (Figures 6a and c); the expression level of pyroptosis proteins in lung tissue was significantly different, respectively, in three different groups at 12, 24, and 48 h (Figure 6d). Based on these results, we found that M2 macrophage polarization induced by rTsP53 suppressed the lung tissue pyroptosis then alleviating ALI.

Discussion

In this study, we investigated the protective effects of rTsP53, the major component of the excretory-secretory antigen of *T. spiralis*, on ALI mice and explored the underlying mechanism of its immune-
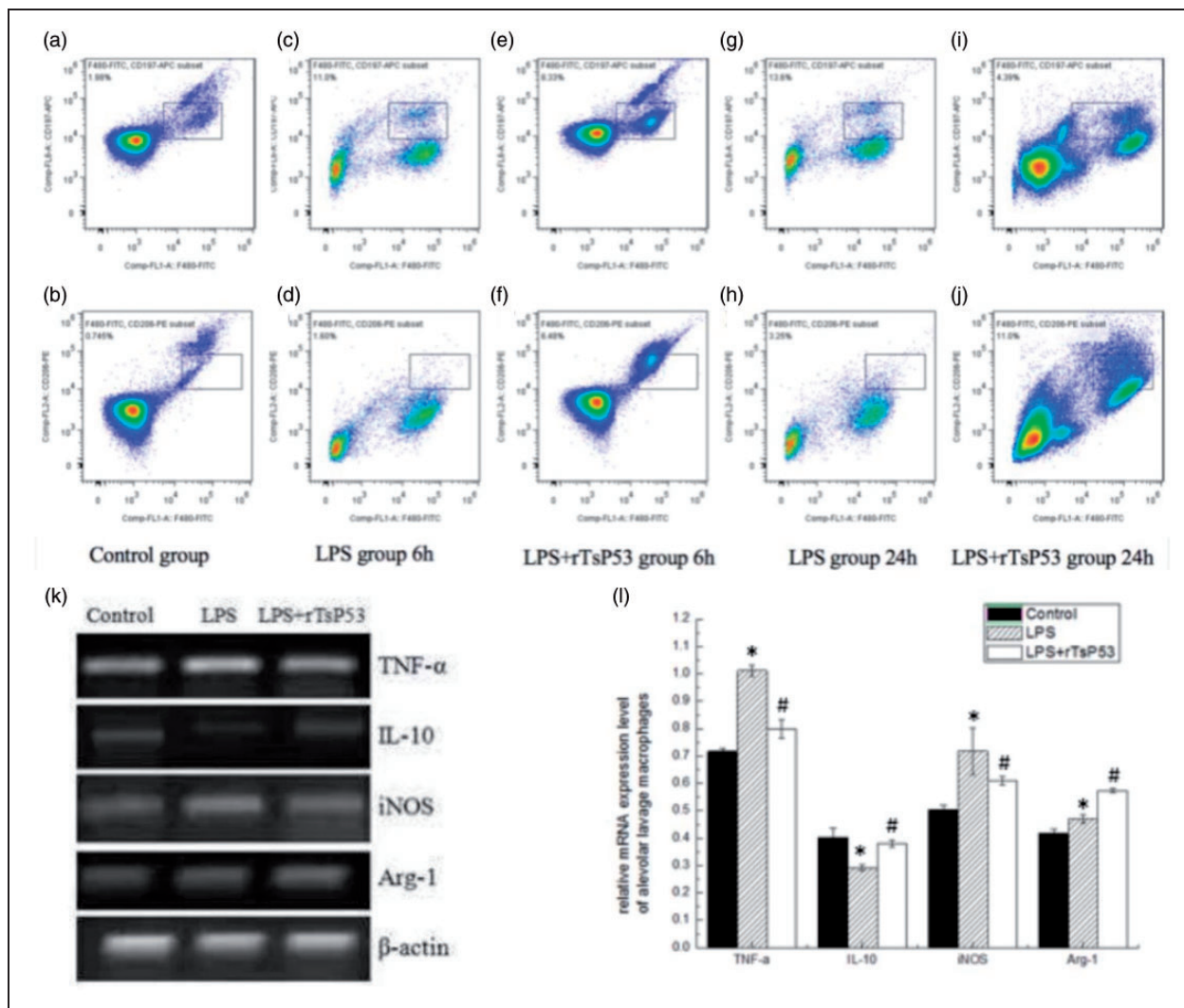
Figure 5. Effect of rTsP53 treatment on macrophages marker and cytokine expression in BALF macrophages from three groups. (a, b) Percentage of F4/80(+)/CD197(+) and F4/80(+)/CD206(+) macrophages was detected in control group. (c, d) Percentage of F4/80(+)/CD197(+) and F4/80(+)/CD206(+) macrophages was detected in LPS group at 6 h. (e, f) Percentage of F4/80(+)/CD197(+) and F4/80(+)/CD206(+) macrophages was detected in LPS + rTsP53 group at 6 h. (g, h) Percentage of F4/80(+)/CD197(+) and F4/80(+)/CD206(+) macrophages was detected in LPS group at 24 h. (i, j) Percentage of F4/80(+)/CD197(+) and F4/80(+)/CD206(+) macrophages was detected in LPS + rTsP53 group at 24 h. (k, l) the relative mRNA expression of TNF-α, IL-10, iNOS and Arg-1 was determined by RT-PCR in different groups at 24 h. Values are means ± SEM, *P < 0.005 vs. LPS group; #P < 0.01 vs. LPS 2 h+rTsP53 group. Data were expressed as the means ± SEM. *P < 0.05 vs. control group, #P < 0.05 vs. LPS group.

modulatory properties on the polarization of alternatively activated macrophages, furthermore alleviating pyroptosis of lung tissues. We established the ALI mice model by LPS injection via the tail vein. These mice showed typical pathological features of ALI such as infusive alveoli damage, hyaline membrane formation, and inflammatory cell infiltration. All evaluation parameters, microscopic Smith score, and wet/dry ratio, in rTsP53+LPS mice were significantly lower than those in the LPS group. RTsP53 pre-treatment attenuated the degree of inflammatory damage and

protected organ function, demonstrating its ability to prevent ALI caused by LPS injection.

A previous study evaluated the immune-modulatory and anti-inflammatory potential of specific *T. spiralis* excretory-secretory components, such as 45, 49, and 53 kDa proteins.[20] We demonstrated that rTsP53 protein attenuated inflammatory damage in the colon tissues of colitis mice by down-regulating pro-inflammatory cytokine expression.[18] Chen et al. suggested that the *T. spiralis* 53-kDa protein decreases the serum levels of inflammatory cytokines IL-6, IFN-γ, and TNF-α
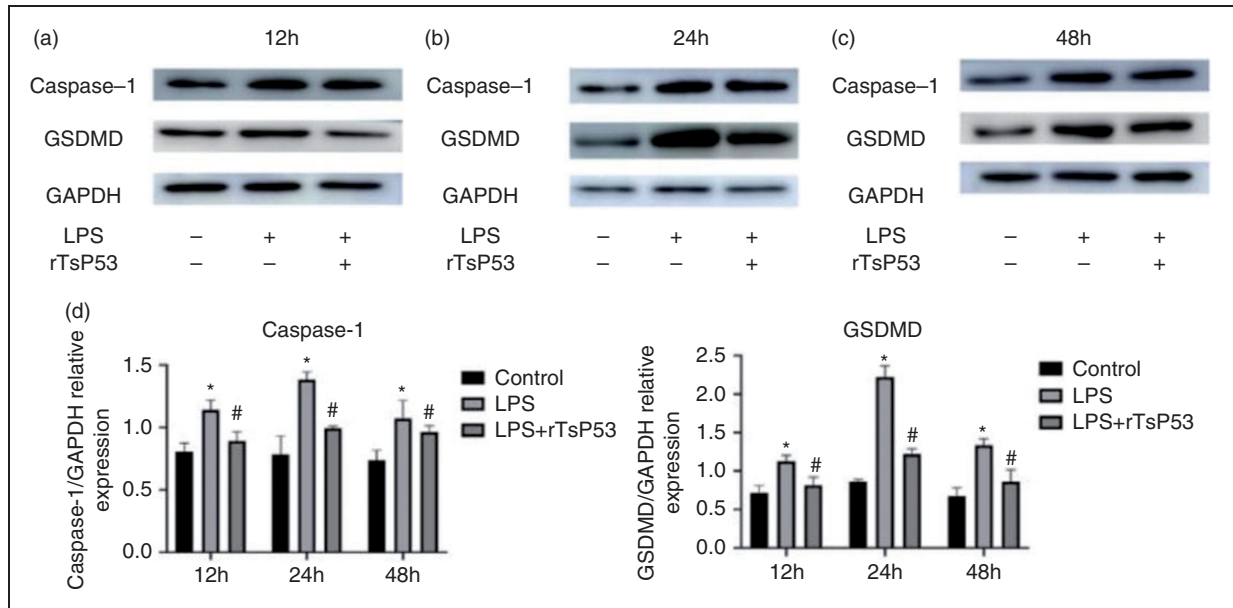
Figure 6. (a–c) RTs-P53 protein suppressed the expression of pyroptosis proteins in lung tissue from different groups at 12 (a), 24 (b), and 48 h (c). (d) Data are expressed as the means ± SEM. *$P < 0.05$ vs. control group, #$P < 0.05$ vs. LPS group.

and attenuates LPS-induced damage during the pro-inflammatory stage of sepsis.[19] Explosive inflammation played a vital role in the pathogenesis and progression of ALI. We verified that rTsP53 downregulated the release of the Th1 cytokines IL-1β, IL-6, and TNF-α and increased the levels of the Th2 cytokines IL-4, IL-10, and IL-13. Additionally, rTsP53 was found to be a strong immune-modulatory agent based on its striking antigenicity in simulating strong IgG1, but not IgG2a, without the use of adjuvant. RTsP53 treatment reduced LPS-induced lung pathological injury, down-regulated pro-inflammatory mediators, and up-regulated anti-inflammatory mediators. IL-4, IL-10, and IL-13 were robust stimulating factors that switch activated B cells to the IgG1 isotype; IL-1β, IL-6, and TNF-α were considered as Th1 type cytokines because they enhanced IgG2a Ab.[20,21] Because rTsP53 protein strongly exhibited Th2-prone immune, significantly up-regulated Th2 cytokines IL-4, IL-10, and IL-13. Then the stimulating factors switched activated B cells to IgG1 isotype. Th2-prone immune status also influenced the phenotype and function of immune cells such as macrophages.[22–24] In this study, we focused on alveolar macrophages, which were key in the pulmonary inflammatory immune response.[25] In the early stage of ALI, classic activated macrophages (M1) marked with CD80 and CD197 were activated by LPS, bacterial products, and Th1-type cytokines and released a variety of chemotactic factors and cytokines such as TNF-α, IL-6, and IL-1β. These cytokines promoted neutrophil cell aggregation and activation, initiating the process of ALI.[26] Tissue factor and inhibitor

of plasminogen activators, also produced by M1 macrophages, accelerated the process of coagulation.[27] In contrast, alternatively activated macrophages (M2) marked with CD163 and CD 206 removed alveolar exudate and released platelet-derived growth factor, TGF-β, and insulin growth factor, which played a role in inflammation alleviation and lung tissue fibrosis in the terminal process of ALI.[28,29] In this study, we used rTsP53 as an immune-modulator to induce the polarization of M2 macrophages from BALF before ALI induced by LPS administration. In the rTsP53+LPS group, we detected higher mRNA expression levels of the M2 marker Arg-1 and anti-inflammatory cytokine IL-10 compared with the LPS group. Arg-1 and iNOS from macrophages controlled NO production by competing for the common substrate L-arginine. Arg-1 was the counter-regulatory enzyme of iNOS and suppressed NO production. Thus, the mRNA expression level of iNOS, an M1 marker, was much lower in the rTsP53 group. Arg-1 was also found to play a role in tissue repair and has been implicated in anti-nematode effects.[30,31] Arg-1 and iNOS were not only markers of the activation of different macrophages, but also involved in pathogen recognition, inflammation reactions, and tissue damage or repair. Thus, rTsP53 may up-regulate M2 to exert these functions. Polarization of M2 in the rTsP53+LPS group was also observed directly by FACS analysis using the marked molecule F4/80(+)/CD206(+). These results provided a theoretical basis for treatment of early-phase ALI by up-regulating M2 macrophages by rTsP53 protein.

The therapeutic effect of rTsP53 reached an early peak about 24 h, then promoting M2 macrophage polarization and reducing pro-inflammatory factor expression (IL-6, TNF-α, and IL-1β), which significantly alleviated LPS-induced ALI. After 24 h, the protective effects of rTsP53 may be based on the anti-inflammatory cytokines produced by M2 macrophage polarization, which has been regarded as an important way to repair the injury lung tissue.[6]

Pyroptosis mediated by inflammatory caspases played an important role in innate immune defense against intracellular bacteria and endotoxin. It is characterized by lytic cell death induced by the binding of intracellular LPS to caspase-1, leading to GSDMD-induced pore formation and the IL-1β release.[32] Unfettered pyroptosis could induce multi-organ injury, including ALI.[33,34] Targeting caspase-activated pyroptosis might be a useful strategy for limiting lung tissue damage. Different phenotypes of macrophage have been shown to be associated with tissue pyroptosis. Recent studies found that M1 macrophage polarization was closely related to pyroptosis in adipose tissue. The experimental evidence showed that LPS could promote the process from the M2 to the M1 phenotype then enhancing adipose tissue pyroptosis.[35] Anti-inflammatory M2 macrophages reduced inflammation-induced myocardial tissue pyroptosis in doxorubicin-induced cardiomyopathy mice.[36] The relationship between phenotypes of macrophage and lung pyroptosis was poorly understood. In the present study, we found that LPS promoted the M1 polarization with elevated expression of pyroptosis proteins, such as caspase-1 and GSDMD, from lung tissue in LPS-induced ALI mice. In addition, rTsP53 protein induced the polarization of M2 macrophages and alleviated the lung tissue pyroptosis demonstrated as significantly decreased protein expression of caspase-1, GSDMD in rTsP53+LPS group. Therefore, there was a correlation between M2 polarization and alleviated lung tissue pyrotopsis. In conclusion, the recombinant 53-kDa protein of *T. spiralis* in mice may protect lung injury via reducing lung tissue pyroptosis by promoting M2 macrophage polarization. The specific mechanism between macrophage polarization and lung pyroptosis remains unclear, which deserves further investigation. The uncertain relationship between rTsP53, M2 macrophage and Lung pyroptosis is a limitation inherent to the research.

Declaration of conflicting interests

The author(s) declared no potential conflicts of interest with respect to the research, authorship, and/or publication of this article.

ORCID iD

Jia Xu https://orcid.org/0000-0001-9869-1820

References

1. Xu H, Xie J, Lei Y, et al. Anti-inflammatory effects of penehyclidine hydrochloride on acute respiratory distress syndrome in rats [in Chinese]. *Zhonghua Wei Zhong Bing Ji Jiu Yi Xue* 2018; 30(8): 764–767.

2. Matthay MA, Ware LB, Zimmerman GA. The acute respiratory distress syndrome. *J Clin Invest* 2012; 122(8): 2731–2740.

3. Malaviya R, Sunil VR, Venosa A, et al. Macrophages and inflammatory mediators in pulmonary injury induced by mustard vesicants. *Ann N Y Acad Sci* 2016; 1374(1): 168–175.

4. Mantovani A, Biswas SK, Galdiero MR, et al. Macrophage plasticity and polarization in tissue repair and remodelling. *J Pathol* 2013; 229(2): 176–185.

5. Lu HL, Huang XY, Luo YF, et al. Activation of M1 macrophages plays a critical role in the initiation of acute lung injury. *Biosci Rep* 2018; 38(2): BSR20171555.

6. Huang X, Xiu H, Zhang S, et al. The role of macrophages in the pathogenesis of ALI/ARDS. *Mediators Inflamm* 2018, 2018: 1264913.

7. Shi J, Gao W, Shao F. Pyroptosis: gasdermin-mediated programmed necrotic cell death. *Trends Biochem Sci* 2017; 42(4): 245–254.

8. Liu X, Zhang Z, Ruan J, et al. Inflammasome-activated gasdermin D causes pyroptosis by forming membrane pores. *Nature* 2016; 535(7610): 153–158.

9. He Y, Hara H, Núñez G. Mechanism and regulation of NLRP3 inflammasome activation. *Trends Biochem Sci* 2016; 41(12): 1012–1021.

10. Horng T. Calcium signaling and mitochondrial destabilization in the triggering of the NLRP3 inflammasome. *Trends Immunol* 2014; 35(6): 253–261.

11. Sauler M, Bazan IS, Lee PJ. Cell death in the lung: the apoptosis-necroptosis axis. *Annu Rev Physiol* 2019; 81: 375–402.

12. Cheng KT, Xiong S, Ye Z, et al. Caspase-11-mediated endothelial pyroptosis underlies endotoxemia-induced lung injury. *J Clin Invest* 2017; 127(11): 4124–4135.

13. Nyiramana MM, Cho SB, Kim EJ, et al. Sea hare hydrolysate-induced reduction of human non-small cell lung cancer cell growth through regulation of macrophage polarization and non-apoptotic regulated cell death pathways. *Cancers (Basel)* 2020; 12(3): 726.

14. Huang X, Xiu H, Zhang S, et al. The role of macrophages in the pathogenesis of ALI/ARDS. *Mediators Inflamm* 2018; 2018: 1264913.

15. Singla DK, Johnson TA, Tavakoli Dargani Z. Exosome treatment enhances anti-inflammatory M2 macrophages and reduces inflammation-induced pyroptosis in doxorubicin-induced cardiomyopathy. *Cells* 2019; 8(10): 1224.

16. Okada H, Ikeda T, Kajita K, et al. Effect of nematode Trichinella infection on glucose tolerance and status of macrophage in obese mice. *Endocr J* 2013, 60(11): 1241–1249.

17. Chen Z, Li F, Yang W, et al. Effect of rTsP53 on the M1/M2 activation of bone-marrow derived macrophage in vitro. *Int J Clin Exp Pathol* 2015; 8(10): 13661–13676.

18. Du L, Tang H, Ma Z, et al. The protective effect of the recombinant 53-kDa protein of Trichinella spiralis on experimental colitis in mice. *Dig Dis Sci* 2011; 56(10): 2810–2817.

19. Chen ZB, Tang H, Liang YB, et al. Recombinant *Trichinella spiralis* 53-kDa protein activates M2 macrophages and attenuates the LPS-induced damage of endotoxemia. *Innate Immun* 2016; 22(6): 419–432.

20. Chakir H, Wang H, Lefebvre DE, et al. T-bet/GATA-3 ratio as a measure of the Th1/Th2 cytokine profile in mixed cell populations: predominant role of GATA-3. *J Immunol Methods* 2003; 278(1–2): 157–169.

21. Rengarajan J, Szabo SJ, Glimcher LH. Transcriptional regulation of Th1/Th2 polarization. *Immunol Today* 2000; 21(10): 479–483.

22. Liu YC, Zou XB, Chai YF, et al. Macrophage polarization in inflammatory diseases. *Int J Biol Sci* 2014; 10(5): 520–529.

23. Shono J, Sakaguchi S, Suzuki T, et al. Preliminary time-course study of antiinflammatory macrophage infiltration in crush-injured skeletal muscle. *Anim Sci J* 2013; 84(11): 744–750.

24. Martinez FO, Helming L, Gordon S. Alternative activation of macrophages: an immunologic functional perspective. *Annu Rev Immunol* 2009; 27: 451–483.

25. Zhao RC, Liao L, Han Q. Mechanisms of and perspectives on the mesenchymal stem cell in immunotherapy. *J Lab Clin Med* 2004; 143(5): 284–291.

26. Lomas-Neira J, Chung CS, Perl M, et al. Role of alveolar macrophage and migrating neutrophils in hemorrhage-induced priming for ALI subsequent to septic challenge. *Am J Physiol Lung Cell Mol Physiol* 2006; 290(1): L51–L58.

27. Chimenti L, Camprubí-Rimblas M, Guillamat-Prats R, et al. Nebulized heparin attenuates pulmonary coagulopathy and inflammation through alveolar macrophages in a rat model of acute lung injury. *Thromb Haemost* 2017; 117(11): 2125–2134.

28. Farley KS, Wang LF, Law C, et al. Alveolar macrophage inducible nitric oxide synthase-dependent pulmonary microvascular endothelial cell septic barrier dysfunction. *Microvasc Res* 2008; 76(3): 208–216.

29. Kambara K, Ohashi W, Tomita K, et al. In vivo depletion of CD206+ M2 macrophages exaggerates lung injury in endotoxemic mice. *Am J Pathol* 2015; 185: 162–171.

30. Witte MB, Barbul A. Arginine physiology and its implication for wound healing. *Wound Repair Regen* 2003; 11(6): 419–423.

31. Anthony RM, Urban JF Jr, Alem F, et al. Memory T(H) 2 cells induce alternatively activated macrophages to mediate protection against nematode parasites. *Nat Med* 2006, 12(8): 955–960.

32. Wallach D, Kang TB, Dillon CP, et al. Programmed necrosis in inflammation: toward identification of the effector molecules. *Science* 2016; 352(6281): aaf2154.

33. Hou L, Yang Z, Wang Z, et al. NLRP3/ASC-mediated alveolar macrophage pyroptosis enhances HMGB1 secretion in acute lung injury induced by cardiopulmonary bypass. *Lab Invest* 2018; 98(8): 1052–1064.

34. Zeng Y, Qin Q, Li K, et al. PKR suppress NLRP3-pyroptosis pathway in lipopolysaccharide-induced acute lung injury model of mice. *Biochem Biophys Res Commun* 2019; 519(1): 8–14.

35. Hersoug LG, Møller P, Loft S. Role of microbiota-derived lipopolysaccharide in adipose tissue inflammation, adipocyte size and pyroptosis during obesity. *Nutr Res Rev* 2018; 31(2): 153–163.

36. Singla DK, Johnson TA, Tavakoli Dargani Z. Exosome treatment enhances anti-inflammatory M2 macrophages and reduces inflammation-induced pyroptosis in doxorubicin-induced cardiomyopathy. *Cells* 2019; 8(10): 1224.